# The changing carbon cycle at Mauna Loa Observatory

**Wolfgang Buermann*†, Benjamin R. Lintner‡§, Charles D. Koven*, Alon Angert*¶, Jorge E. Pinzon‖, Compton J. Tucker‖, and Inez Y. Fung*,****

*Berkeley Atmospheric Sciences Center and ‡Department of Geography, University of California, Berkeley, CA 94720; and ‖National Aeronautics and Space Administration/Goddard Space Flight Center, Greenbelt, MD 20771

Contributed by Inez Y. Fung, December 29, 2006 (sent for review July 6, 2006)

**The amplitude of the $CO_2$ seasonal cycle at the Mauna Loa Observatory (MLO) increased from the early 1970s to the early 1990s but decreased thereafter despite continued warming over northern continents. Because of its location relative to the large-scale atmospheric circulation, the MLO receives mainly Eurasian air masses in the northern hemisphere (NH) winter but relatively more North American air masses in NH summer. Consistent with this seasonal footprint, our findings indicate that the MLO amplitude registers North American net carbon uptake during the warm season and Eurasian net carbon release as well as anomalies in atmospheric circulation during the cold season. From the early 1970s to the early 1990s, our analysis was consistent with that of Keeling *et al.* [Keeling CD, Chin JFS, Whorf TP (1996) *Nature* 382:146–149], suggesting that the increase in the MLO $CO_2$ amplitude is dominated by enhanced photosynthetic drawdown in North America and enhanced respiration in Eurasia. In contrast, the recent decline in the $CO_2$ amplitude is attributed to reductions in carbon sequestration over North America associated with severe droughts from 1998 to 2003 and changes in atmospheric circulation leading to decreased influence of Eurasian air masses. With the return of rains to the U.S. in 2004, both the normalized difference vegetation index and the MLO amplitude sharply increased, suggesting a return of the North American carbon sink to more normal levels. These findings indicate that atmospheric $CO_2$ measurements at remote sites can continue to play an important role in documenting changes in land carbon flux, including those related to widespread drought, which may continue to worsen as a result of global warming.**

atmospheric circulation | atmospheric $CO_2$ seasonal cycle | terrestrial carbon sinks | continental droughts

The time series of $CO_2$ at Mauna Loa Observatory (MLO) located on the Island of Hawaii is unique not only because of its accuracy and length but also because it was designed and has been repeatedly demonstrated to capture the globally averaged secular trend in atmospheric $CO_2$. The seasonal cycle of atmospheric $CO_2$ at the MLO, with a maximum at the beginning of the growing season (May) and a minimum at the end of the growing season (September/October), records the "breathing" of the northern hemisphere (NH) biosphere, that is, the seasonal asynchrony between photosynthetic drawdown and respiratory release of $CO_2$ by terrestrial ecosystems (e.g., refs. 1–3).

During the course of a year, the MLO experiences marked shifts in large-scale atmospheric circulation. In the NH cold season, air masses from Eurasia dominate transport to the MLO as a result of a deepening of the Aleutian Low and intensified midlatitude westerly flow (4). In the NH warm season, the dominant subtropical North Pacific high-pressure system located to the northeast of the MLO leads to short-range transport of air masses to the MLO that originate over or near the North American continent (4). During this season, the MLO receives an approximately equal mix of air masses from both continents with relatively more North American contributions at the peak of the NH growing season (July/August). The MLO is also located in the vicinity of the subsiding branch of the Hadley circulation, rendering it sensitive to interhemispheric mixing.

Several studies have analyzed variability in the MLO $CO_2$ seasonal cycle to infer the sensitivity of ecosystem dynamics to climate perturbations. The increasing trends in the seasonal amplitude of $CO_2$ at the MLO and Point Barrow, AK, from the early 1970s to the early 1990s are postulated to be evidence of a temperature-related lengthening of the boreal growing season (1). Reports of a greening trend in the satellite-derived normalized difference vegetation index (NDVI) throughout the 1980s at northern high latitudes consistent with springtime warming provided additional support for this hypothesis (5). The warming trend at northern high latitudes stimulated wintertime respiration as well as summertime photosynthesis, with both contributing to the observed $CO_2$ amplitude increases (6). In addition to these temperature-based analyses, positive trends in precipitation from 1950 to 1993 over the continental United States have also contributed to higher rates of carbon sequestration (7), consistent with the $CO_2$ record.

An updated analysis of $CO_2$ and climate time series reveals a different picture for the recent decade. Even with some interannual fluctuations, the trend in the Mauna Loa seasonal amplitude since the early 1990s has been negative despite the continued warming over northern latitudes (Fig. 1). In addition, prolonged and spatially extensive midlatitude continental droughts (8) and declines in plant growth (9) were observed from 1998 to 2003. An analysis of the $CO_2$, NDVI, temperature, and precipitation records averaged for the NH shows that since 1994, NH $CO_2$ uptake in the springtime has been accelerating as a result of warming, whereas net $CO_2$ uptake in the summer is lower than in the previous decade because of droughts (10). Because there are no continental-scale observations of respiration, the respiratory release of $CO_2$ is modeled as a function of ambient temperature, soil moisture, and the amount of refractory carbon in litter and soils. Thus, estimates of the net carbon flux (or carbon source/sink) are model-dependent and only weakly constrain explanations of variability and trends in the $CO_2$ amplitude.

Here we analyze the $CO_2$ record at a single station, the MLO, to focus on interannual and quasidecadal changes in carbon

Author contributions: W.B. and I.Y.F. designed research; W.B., B.R.L., C.D.K., and A.A. performed research; W.B., J.E.P., and C.J.T. analyzed data; W.B. and I.Y.F. wrote the paper; and J.E.P. and C.J.T. contributed NDVI data.

The authors declare no conflict of interest.

Freely available online through the PNAS open access option.

Abbreviations: MLO, Mauna Loa Observatory; NH, northern hemisphere; NDVI, normalized difference vegetation index; SPI, standardized precipitation index; PDSI, Palmer drought-severity index.

†To whom correspondence may be sent at the present address: Center for Tropical Research, UCLA Institute of the Environment, P.O. Box 951496, Los Angeles, CA 90025-1496. E-mail: buermann@ucla.edu.

§Present address: Department of Atmospheric and Oceanic Sciences and Institute of Geophysics and Planetary Physics, University of California, Los Angeles, CA 90095.

¶Present address: Department of Environmental Sciences and Energy Research, Weizmann Institute of Science, Rehovot 76100, Israel.

**To whom correspondence may be addressed. E-mail: ifung@uclick.berkeley.edu.

This article contains supporting information online at www.pnas.org/cgi/content/full/0611224104/DC1.

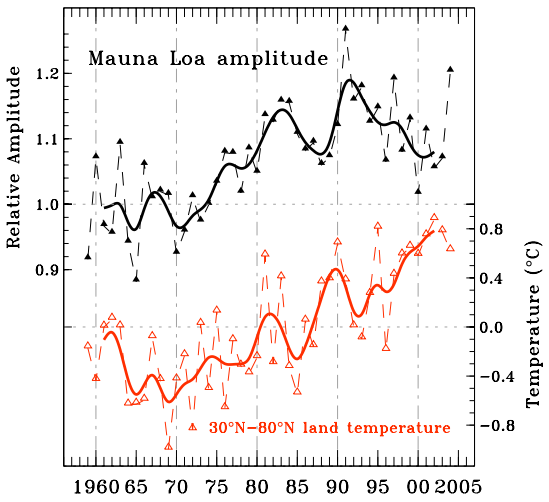


**Fig. 1.** Time series of the relative amplitude of the seasonal cycle of atmospheric $CO_2$ at the MLO (black) and anomalies in observed annual land temperatures (red) for the latitudinal band from 30°N to 80°N (except Greenland). Plotted are both annual means (triangles connected by dashed lines) and a smoothed time series based on a five-point binomial filter (thick solid curves). The relative amplitudes are in respect to the mean amplitude of the first 5 yr of $CO_2$ record (1959–1963). Temperature anomalies are relative to the 1959–2004 study period. For both time series, annual values correspond to the annual tick marks on the time axis.

sources/sinks in North America versus those in Eurasia. The analysis takes advantage of the MLO's changing seasonal footprint from relatively more North American contributions during the NH growing season (May to October) to more Eurasian contributions during the NH cold season (November to April). We present evidence that the observed decline in the MLO seasonal amplitude since the early 1990s is indicative of a slowing North American carbon sink in the growing season as well as changing footprints of atmospheric transport in the cold season. To examine these hypotheses, we analyzed spatial and temporal correlation patterns of the MLO seasonal amplitude time series with gridded fields of the satellite NDVI, land surface temperature, and indices that represent drought as well as outputs from a recent integration of an atmospheric transport model.

## Results

**MLO Amplitude.** An updated record from the MLO indicates that the amplitude of the $CO_2$ seasonal cycle has been declining since the early 1990s at a rate of −0.05 ppm/yr (Fig. 1) despite the continued increasing trend in annual NH land temperatures. The declining trend in the amplitude is statistically significant for the period 1991–2004 ($r = 0.48$, $P < 0.05$).

**Warm-Season Influence.** ***Spatial correlations.*** A spatial correlation analysis between time series of the MLO amplitude and NH growing-season temperatures for the earlier nonsatellite period 1959–1981 reveals largely positive correlations over western North America (Fig. 2*a*). There are no significant amplitude–temperature correlations over Eurasia. The amplitude correlation with the 6-month standardized precipitation index (SPI6) averaged over the growing season shows no significant geographically extensive pattern for this earlier period (Fig. 2*b*). The sign of the amplitude–temperature correlations is such that warmer (cooler) conditions are associated with larger (smaller) amplitudes, consistent with the hypothesis of temperature-related changes in plant activity during the growing season (1).

For the later satellite period 1982–2004, the amplitude–temperature correlations over western North America are opposite in sign to the earlier period; moreover, the region of significant correlation is shifted toward lower latitudes (Fig. 2*c*). In this period, the temperature correlations are colocated with those of SPI6, with the sign such that warmer and drier conditions correspond to smaller amplitudes (Fig. 2 *c* and *d*). Satellite measurements of the NDVI allow direct estimation of photosynthetic activity. The spatial correlations of the MLO amplitude and growing-season NDVI for 1982–2004 identify the midlatitudes in general, and North America in particular, as regions of common variability (Fig. 2*e*). A comparison with the corresponding growing-season temperature and SPI6 patterns shows that regions that exhibit strong correlations with the MLO amplitude are colocated with those for the NDVI especially over western North American midlatitudes (Fig. 2 *c*–*e*). The sign of the correlations is such that greener (browner), wetter (drier), and cooler (warmer) conditions correspond to larger (smaller) am-

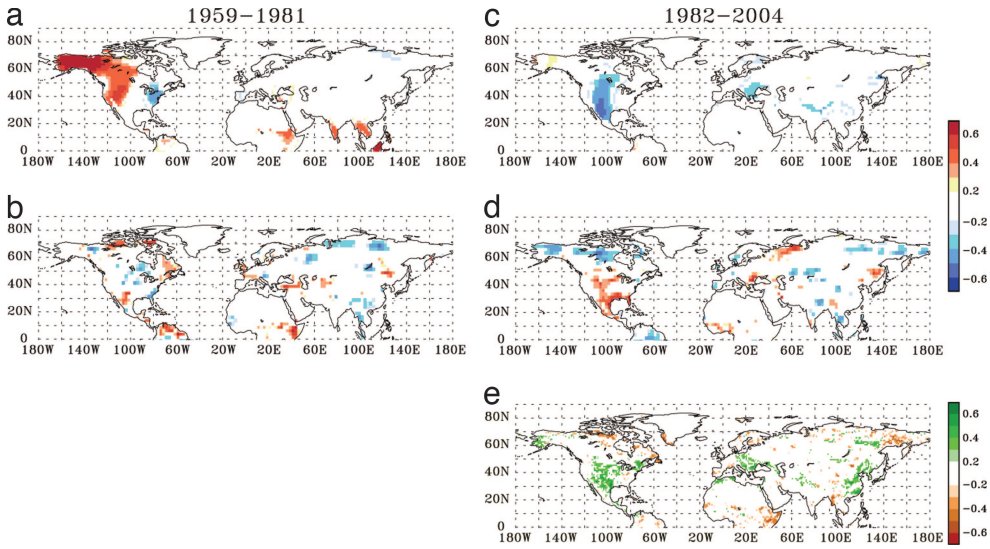


**Fig. 2.** Correlations of the MLO amplitude time series with mean growing-season (May to October) climate and NDVI gridded fields for two 23-yr study periods: 1959–1981 (*a* and *b*) and 1982–2004 (*c*–*e*). The maps show correlation patterns for land surface temperature (*a* and *c*), SPI6 (*b* and *d*), and NDVI (*e*). Contoured are only correlations that are statistically significant at the 90% level ($r \geq 0.28$; Student's *t* test, one-tailed).

plitudes. Thus, our results show that the MLO amplitude changes since 1982 are also dominated by changes in photosynthesis in North America, but in this period they are dominated by moisture-related variability in photosynthesis.

The regions of influence in North America largely encompass the vast grass- and croplands of the Midwestern United States (11), confirming both their vulnerability to drought stress and potential significance in midlatitude carbon-exchange anomalies (12). At grass sites under severe drought conditions, photosynthesis seems to be more impacted relative to respiration (e.g., ref. 13), leading to reduced net $CO_2$ uptake during the growing season and a smaller amplitude. During 1982–2004, photosynthetic changes over far-eastern Eurasia also seem to have contributed to the MLO amplitude variations, although the region of influence is smaller in area when compared with western North America.

In their pioneering study, Keeling *et al.* (1) found the strongest relationship between the MLO amplitude and annually averaged NH land temperatures, with the amplitude lagging temperature by 1 and 2 yr. To account for such behavior, we also computed lagged spatial correlations between the MLO amplitude and NH growing-season NDVI, hydrologic parameters, as well as temperature for the two study periods 1959–1981 and 1982–2004. The results indicate that only in the case of temperature and during the early study period 1959–1981 are significant and spatially extensive 1-yr-lagged correlations evident; the sign of these correlations are positive, and their spatial extent spans the mid-to-high latitudes of eastern Eurasia [see supporting information (SI) *Text* and SI Fig. 6].

***Temporal evolution.*** To understand the temporal behavior of the MLO amplitude, we computed time series of spatial and growing-season means of the NDVI, hydrologic parameters, and temperature over regions that showed significant correlations with the MLO amplitude (compare with Fig. 2). For the NDVI, SPI6, and Palmer drought-severity index (PDSI), these regions include the vegetated portion of the midlatitudes of western North America and far-eastern Eurasia (Fig. 3 *a* and *b*). For temperature, the corresponding spatial correlation patterns are more extensive (compare Fig. 2 and *SI* Fig. 6); consequently, spatial means are calculated over a larger area encompassing the vegetated mid-to-high latitudes of North America and eastern Eurasia (Fig. 3 *c* and *d*).

Over the 46 yr (1959–2004) of observation, growing-season temperatures increased at mean rates of 0.011°C/yr ($r = 0.41$, $P < 0.005$) for North America and 0.021°C/yr ($r = 0.6$, $P < 0.001$) for eastern Eurasia, although the warming has accelerated markedly since the early 1990s over both continents (Fig. 3 *c* and *d*). The summer midlatitude hydrologic regime has different trends between western North America and far-eastern Eurasia, with the SPI6 and PDSI for the period from the early 1960s to the mid-1980s tending toward wetter conditions over western North America (Fig. 3*a*) but only weakly variable conditions over far-eastern Eurasia (Fig. 3*b*). In this earlier period, photosynthetic drawdown in North America was likely enhanced and contributed to the observed increase in the MLO amplitude. From the mid-1980s onward, however, the hydrologic cycle over these midlatitude regions has become much more variable; this is particularly evident for North America with two prolonged droughts (1987–1989 and 1998–2003) and an anomalous wet period in the early 1990s (8, 14). During this period, variability in the MLO amplitude followed closely variations in the North American hydrological and NDVI time series (see also below), lending strong support to the notion that also the recent decline in the MLO amplitude since the early 1990s is, in part, a signature of drought-related decreases in growing-season net carbon uptake.

Changing contributions of the various factors inducing variations in the MLO amplitude are seen in their 11-yr moving-window correlations with the MLO amplitude (Fig. 3 *Lower*).

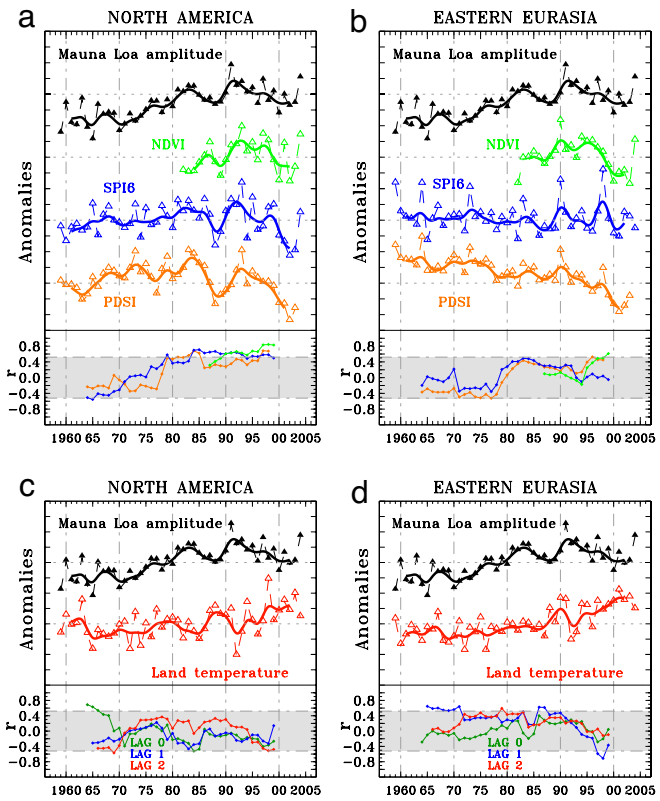


**Fig. 3.** Standardized anomalies in the MLO amplitude (black) and spatial averages of mean growing-season (May to October) NDVI (green), SPI6 (blue), PDSI (orange), and temperature (red), and moving-window correlations between these indices and the MLO amplitude. (*Upper*) For the NDVI, SPI6, and PDSI, the spatial averaging was performed from 20°N to 50°N and 90°W to 120°W for North America (*a*) and 20°N to 50°N and 100°E to the eastern coast for Eurasia (*b*). For temperature, the spatial averaging domain spans 30°N to 80°N for North America (*c*) and from 30°N to 80°N and 60°E to the eastern coast for Eurasia (*d*). Nonvegetated areas were masked out in the spatial averaging. Positive anomalies in SPI6 and PDSI indicate wetter conditions, whereas those in the NDVI and temperature correspond to greener and warmer conditions. For *a* and *b*, all standardized anomalies are relative to the 1982–2004 period of the NDVI satellite record, whereas for *c* and *d*, the standardized anomalies are relative to 1959–2004. Plotted are both annual values (triangles connected by dashed lines) and a smoothed curve based on a five-point binomial filter (thick solid curves). One tick mark on the *y* scale corresponds to 1 SD. (*Lower*) The window length for the moving correlations between amplitude and the corresponding climate and the NDVI indices is 11 yr, and the corresponding correlation is plotted in the middle (year 6) of each interval (diamonds). For *a* and *b*, the moving correlations between the amplitude and the indices are plotted by using the same color assignments as in *Upper*. For *c* and *d*, moving correlations between amplitude and temperature are shown for zero (green) and 1-yr (blue) and 2-yr (red) lags, with the amplitude always lagging. Nonshaded correlations are statistically significant at the 95% level ($r \geq 0.52$; Student's *t* test, one-tailed).

Warm-season temperatures over North America (zero lag) and eastern Eurasia (1-yr lag) show some persistent positive correlation with the MLO amplitude from the beginning of the record until approximately the mid-1970s but little thereafter (Fig. 3 *c Lower* and *d Lower*). Moving-window correlations with the North American NDVI and hydrologic time series show that the correlations become significant with the onset of a more rigorous hydrological cycle in the early 1980s (Fig. 3*a Lower*). For far-eastern Eurasia, on the other hand, the moving correlations between the MLO amplitude and NDVI as well as PDSI approach significance only when the most recent pronounced drought period is enclosed (Fig. 3*b Lower*). The strong amplitude

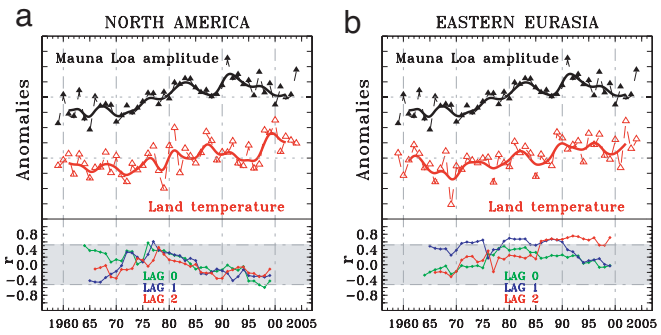


**Fig. 4.** Standardized anomalies in the MLO amplitude (black) and spatial averages of mean cold-season (November to April) temperature (red) and corresponding moving-window correlations. (*Upper*) The temperature spatial means encompass 30°N to 80°N for North America (*a*) and 30°N to 80°N and 60°E to the eastern coast for Eurasia (*b*). Nonvegetated areas were masked out in the spatial averaging. All standardized anomalies are relative to the whole study period, 1959–2004. Plotted are both annual values (triangles connected by dashed lines) and a smoothed curve based on a five-point binomial filter (thick solid curves). One tick mark on the *y* scale corresponds to 1 SD. (*Lower*) The window length for the moving correlations between amplitude and the temperature time series is 11 yr, and the respective correlation is plotted in the middle (year 6) of each interval (diamonds). Moving correlations between amplitude and temperature are shown for zero (green) and 1-yr (blue) and 2-yr (red) lags, with the amplitude always lagging. Nonshaded correlations are statistically significant at the 95% level ($r \geq 0.52$; Student's *t* test, one-tailed).

correlations with both PDSI and NDVI time series for western North America during the drought-prone recent decade underscore the importance of both precipitation (moisture supply) and evapotranspiration (moisture demand) in influencing soil moisture availability, photosynthesis, and carbon uptake.

**Cold-Season Influence.** ***Spatial correlations.*** Another possible contributor to changes in the MLO $CO_2$ amplitude is changes in cold-season heterotrophic respiration, which responds principally to temperature and litter variability over several years. Thus, we also computed zero and lagged spatial correlations between the MLO amplitude and NH cold-season temperatures for the two study periods of 1959–1981 and 1982–2004 (see *SI Text* and SI Fig. 7). The results indicate weak correlations at zero lag over high-latitude North America for 1959–1981 and significant spatially extensive correlations at 1- and 2-yr lags over the mid-to-high latitudes of predominantly eastern Eurasia for both study periods. The sign of these correlations are positive and in the Eurasian case, their spatial extent varies somewhat for the two study periods (see SI Fig. 7).

***Temporal evolution.*** The amplitude–temperature spatial correlations for the NH warm and cold seasons at zero (North America) and various (Eurasia) lags, if present, encompass similar regions (Fig. 2 and *SI Text*). Hence, we computed time series of spatial means of cold-season temperature over the same areas as in the warm-season analysis for studying temporal correlations with the MLO amplitude (Fig. 4). In comparison to the trends in warm-season temperatures, cold-season temperatures averaged over vegetated North America and eastern Eurasia have increased more rapidly over the entire study period (1959–2004) at mean rates of 0.033°C/yr ($r = 0.54$, $P < 0.001$) and 0.038°C/yr ($r = 0.51$, $P < 0.001$), respectively.

Moving-window correlations suggest that there is no evidence of persistent correlations between MLO amplitude and North American cold-season temperatures (Fig. 4*a Lower*). In contrast, persistent correlations do exist between MLO amplitude and cold-season temperatures averaged over eastern Eurasia, but their temporal evolution is complex (Fig. 4*b Lower*). Over the entire study period, Eurasian cold-season temperatures and MLO amplitude at zero lag are not significantly correlated, suggesting that temperature variations by themselves do not dominate variations in respiration rates that influence the MLO amplitude. With MLO amplitude at 1-yr lag, a relatively persistent positive correlation is found from the late 1960s to the early 1990s, the time of common upward trends in both of these time series; thereafter, this 1-yr-lagged relationship becomes insignificant. At 2-yr lag, a significant positive correlation is found to emerge in the early 1980s and persists to the end of the record. This correlation is dominated by interannual fluctuations and not by the trends in temperatures (see *SI Text* and SI Table 1), because the MLO amplitude has declined since the early 1990s, whereas eastern-Eurasian cold-season temperatures have remained relatively flat over this time period (Fig. 4*b*).

During the first half of the satellite period (1982–1993), the warming trends in eastern-Eurasian cold- and warm-season temperatures (Figs. 3*d* and 4*b*) seem to have increased the amount of refractory litter, as suggested by parallel trends in the NDVI (see *SI Text* and SI Fig. 8), and have enhanced decomposition in subsequent years, contributing to a larger amplitude. In contrast, increasing summer drought stress during the most recent decade (11) seems to have weakened the positive linkage between temperature and NDVI, and the NDVI time series has remained relatively flat (see SI Fig. 8). This diverging behavior suggests that the MLO amplitude decline since the early 1990s is not capturing any trends in cold-season decomposition related to the production of refractory litter.

The complex relationship between Eurasian cold-season temperature and the MLO amplitude illustrates the multifaceted controls on winter decomposition (15). For example, at a black spruce forest in Manitoba, Canada, respiration rates from soil carbon reservoirs were found to be sensitive to the depth and duration of thaw (16). It is possible that a similar freeze–thaw mechanism gained significance at a larger spatial scale in the mid- to late 1980s as a result of the massive mid- to high-latitude winter warming over eastern Eurasia in this time frame (Fig. 4*b*). Such a mechanism could partially explain the observed changes in the lagged MLO amplitude responses: a lagged response may develop as decomposition of soil carbon pools is initially inhibited with the onset of thawing and saturation of soils but resumes as soils become gradually drier.

**Circulation Variability.** The generally stronger correlations between the MLO amplitude and North America growing-season climate and NDVI are consistent with the seasonally varying circulation imprint of the MLO (4). Interannual and interdecadal variability in temperature and hydrology is accompanied by shifts in atmospheric circulation that would alter the trajectories of air masses, and hence $CO_2$ amounts, reaching the MLO.

Results from an integration of an atmospheric transport model forced with constant biospheric and fossil-fuel fluxes but interannually changing winds over the period of 1972–2003 (4) suggest that, in the 1990s, less fossil-fuel $CO_2$ was transported to the MLO during the NH spring (see also Fig. 5). Transport anomalies also seem to have decreased the total (biospheric + fossil fuel) simulated $CO_2$ concentrations at the MLO during this time of the year in the 1990s (4) and, consequently, the simulated amplitude (Fig. 5). Observations of radon-222 at the MLO (17, 18) are consistent with these findings and suggest a reduction in continental (Eurasian-originating) airflow at the beginning of the growing season from the early to the mid-1990s (Fig. 5). Indeed, a decrease in continental airflow toward the MLO in the NH spring would lower the maximum concentrations of the $CO_2$ seasonal cycle and, hence, reduce the amplitude.

## Discussion and Summary

The unique location of the MLO in the context of seasonally varying atmospheric circulation allows the separate identifica-

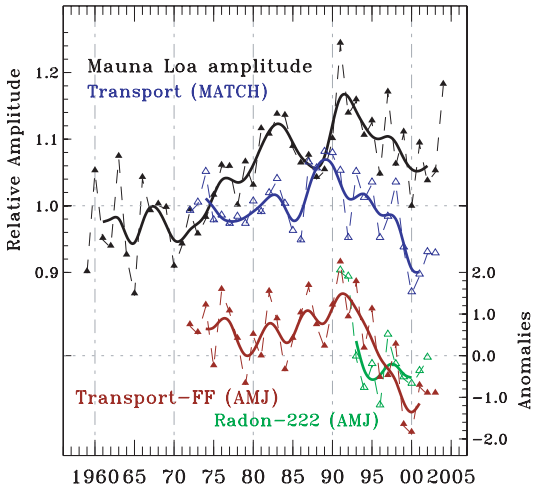


**Fig. 5.** Time series of observed (black) and simulated (blue) relative amplitude of the seasonal cycle of atmospheric $CO_2$ at the MLO, and standardized anomalies in mean springtime (April to June) simulated fossil fuel (FF) only (dark red) and observed radon-222 (green) concentrations. Plotted are both annual (dashed) and 5-yr running (thick line) means. Following ref. 4, simulated monthly $CO_2$ concentrations from the transport-model (MATCH) output correspond to three vertical and nine horizontal grid-point averages centered at the MLO station (155°W, 19°N). For consistency, the seasonal cycle from the monthly MATCH record was extracted with the same curve-fitting algorithm that was used for the observed record (see *Methods*). The observed and simulated relative amplitudes are in respect to the corresponding mean amplitude of the first 5 yr of simulations (1972–1976). Simulated FF and radon anomalies are relative to the 1992–2002 radon record.

tion of the variations in North American versus Eurasian carbon sources and sinks. Our analysis of the increasing trend in the MLO amplitude from the early 1970s to the early 1990s extends the analysis of Keeling *et al.* (1) by attributing the photosynthetic drawdown to North America and enhanced cold-season respiration to Eurasia. The time series of the MLO amplitude beyond the early 1990s shows behavior and controls very different from the earlier two decades. Our analysis suggests that throughout the last two decades, the MLO $CO_2$ seasonal amplitude has recorded a changing North American carbon sink that is dominated by shifts in the North American hydrologic regime rather than by temperature trends. The decline in the MLO amplitude since the early 1990s captures the effects of North American droughts, especially those of 1998–2003, on growing-season carbon uptake on the continent. The amplitude decline is also attributed to reduced cold-season $CO_2$ transport from Eurasia in the early 1990s arising from changes in large-scale atmospheric circulation, especially in the NH spring.

Inversion and ecosystem models have inferred significant and variable Eurasian and North American carbon sinks for the past two decades (e.g., refs. 10, 19, and 20). The analysis of the MLO amplitude variations here supports the inversion result of a stronger North American net carbon uptake during 1991–1995 compared with 1988–1990. The MLO amplitude provides little constraint on the inferred Eurasian carbon sink because the MLO does not capture a strong signature of Eurasian net photosynthesis, given that Eurasian-originating air masses arriving at the MLO dominate in the cold season but not the growing season.

With the return of rains to the US in 2004, the MLO amplitude sharply increased, suggesting a return of the North American carbon sink to more normal levels. The latter emphasizes the exquisite sensitivity of the North American terrestrial carbon sink to changes in the hydrologic regime. This work suggests that time-series measurements of atmospheric $CO_2$ at remote sites can continue to play an important role in documenting changes in land-carbon flux, including those related to widespread drought, which future projections (e.g., refs. 21 and 22) show may continue to worsen as a result of global warming.

## Methods

**$CO_2$ Data.** For this study, monthly averaged atmospheric $CO_2$ concentrations at the MLO, based on *in situ* air samples, from 1959 to 2004 were obtained from the Carbon Dioxide Information Analysis Center (23). The only missing 3-month data period from February to April in 1964 was filled by linear interpolation between the January and May concentrations of that year.

**NDVI Data.** For global vegetation, we used an improved and extended version of the National Aeronautics and Space Administration Global Inventory Modeling and Mapping Studies monthly NDVI data set at 1° spatial resolution spanning the period 1982–2004 (24, 25). The NDVI is computed as the difference between near-infrared and red reflectance of the land surface, normalized by the sum of the reflectances, and is indicative of photosynthetic activity (26).

**Climate Data.** The climate data used in this study include an updated version of the monthly Goddard Institute for Space Studies land temperature data at 2° × 2° spatial resolution (27), as well as the monthly Climate Prediction Center precipitation reconstruction land data at 2.5° × 2.5° spatial resolution (28). To represent anomalies in moisture supply, we computed a SPI (29), defined as the precipitation anomaly over a specified time period leading up to and including the month of interest normalized by its SD. For this study, we computed a 6-month SPI (SPI6) for each month on the basis of the 1959–2004 precipitation record, because the variability in moisture supply at this time scale compares well with variations in seasonal vegetation productivity (30).

In addition to the SPI, we used a monthly PDSI data set at 2.5° × 2.5° spatial resolution (31). The PDSI also incorporates moisture demand via surface temperature, in contrast to the SPI that is based on observed moisture supply alone.

**Data Analysis.** To extract the seasonal cycle from the monthly $CO_2$ record, we applied the curve-fitting procedures (the CCGVU software) developed at the National Oceanic and Atmospheric Administration Climate Monitoring and Diagnostics Laboratory (32). A brief description of the procedure and applied parameters can be found in *SI Text*. For the MLO, all annual maximum concentrations in the seasonal cycle were recorded in the month of May, whereas the minimum concentrations shifted between September and October. The annual MLO amplitude is computed by subtracting the annual minimum from the annual maximum of the seasonal cycle.

The analysis is carried out for the NH warm season (May to October) when photosynthesis exceeds respiration and for the preceding NH cold season (November to April) when heterotrophic respiration dominates the $CO_2$ flux to the atmosphere. In the spatial correlation analysis, the 46-yr study period is separated into two 23-yr episodes, 1959–1981 and 1982–2004, with the satellite NDVI being available only for the latter period.

This article is dedicated to the memory of Dr. Charles D. Keeling. This study was supported by the National Oceanic and Atmospheric Administration, National Aeronautics and Space Administration Carbon Program Grant NAG5-11200, and National Aeronautics and Space Administration EOS-IDS Grant NAG5-9514.

1. Keeling CD, Chin JFS, Whorf TP (1996) *Nature* 382:146–149.
2. Fung I, Tucker CJ, Prentice KC (1987) *J Geophys Res Atmos* 92:2999–3015.
3. Randerson JT, Thompson MV, Conway TJ, Fung IY, Field CB (1997) *Global Biogeochem Cycles* 11:535–560.

4. Lintner B, Buermann W, Koven C & Fung. I. Y (2006) *J Geophys Res Atmos*, doi:10.1029/2005JD006535.
5. Myneni RB, Keeling CD, Tucker CJ, Asrar G, Nemani RR (1997) *Nature* 386:698–702.
6. Randerson JT, Field CB, Fung IY, Tans PP (1999) *Geophys Res Lett* 26:2765–2768.
7. Nemani R, White M, Thornton P, Nishida K, Reddy S, Jenkins J, Running S (2002) *Geophys Res Lett*, doi:10.1029/2002GL014867.
8. Hoerling M, Kumar A (2003) *Science* 299:691–694.
9. Lotsch A, Friedl MA, Anderson BT, Tucker CJ (2005) *Geophys Res Lett*, doi:10.1029/2004GL022043.
10. Angert A, Tucker CJ, Biraud S, Bonfils C, Henning CC, Buermann W, Fung I (2005) *Proc Natl Acad Sci USA* 102:10823–10827.
11. Friedl MA, McIver DK, Hodges JCF, Zhang XY, Muchoney D, Strahler AH, Woodcock CE, Gopal S, Schneider A, Cooper A, *et al.* (2002) *Rem Sens Environ* 83:287–302.
12. Novick KA, Stoy PC, Katul GG, Ellsworth DS, Siqueira MBS, Juang J, Oren R (2004) *Oecologia* 138:259–274.
13. Meyers TP (2001) *Agric For Meteorol* 106:205–214.
14. Dai A, Trenberth KE, Karl TR (1998) *Geophys Res Lett* 25:3367–3370.
15. Monson RK, Burns SP, Williams MW, Delany AC, Weintraub M, Lipson DA (2006) *Global Biogeochem Cycles*, doi:10.1029/2005GB002684.
16. Goulden ML, Wofsy SC, Harden JW, Trumbore SE, Crill PM, Gower ST, Fries T, Daube BC, Fan SM, Sutton DJ, *et al*. (1998) *Science* 279:214–217.
17. Hutter AR, Larsen RJ, Maring H, Merrill JT (1995) *J Radioanal Nucl Chem* 193:309–318.
18. Whittlestone S, Zahorowski W (1998) *J Geophys Res Atmos* 103:16743–16751.
19. Bousquet P, Peylin P, Ciais P, Le Quere C, Friedlingstein P, Tans PP (2000) *Science* 290:1342–1346.
20. Roedenbeck C, Houweling S, Gloor M, Heimann M (2003) *Atmos Chem Phys* 3:1919–1964.
21. Trenberth KE, Dai A, Rasmussen RM, Parsons DB (2003) *Bull Am Meteorol Soc* 84:1205–1217.
22. Fung I, Doney SC, Lindsay K, John J (2005) *Proc Natl Acad Sci USA* 102:11201–11206.
23. Keeling CD, Whorf TP (2004) in *A Compendium of Data on Global Change*, eds Carbon Dioxide Information Analysis Center (Oak Ridge National Laboratory, Oak Ridge, TN).
24. Tucker CJ, Pinzon JE, Brown ME, Slayback D, Pak EW, Mahoney R, Vermote E, Saleous NE (2005) *Int J Remote Sens* 26:4485–4498.
25. Pinzon J, Brown ME, Tucker CJ (2005) in *Hilbert-Huang Transform*: *Introduction and Applications*, eds Huang NE, Shen SS (World Scientific, Singapore), pp 167–186.
26. Myneni RB, Hall FG, Sellers PJ, Marshak AL (1995) *IEEE Trans Geosci Remote Sens* 33:481–486.
27. Hansen J, Ruedy R, Glascoe J, Sato M (1999) *J Geophys Res Atmos* 104:30997–31022.
28. Chen M, Xie P, Janowiak JE, Arkin PA (2002) *J Hydrometeorol* 3: 249–266.
29. McKee TB, Doesken NJ, Kleist J (1993) in *Proceedings of the 8th Conference on Applied Climatology* (Am Meteorol Soc, Boston), pp 179–186.
30. Lotsch A, Friedl MA, Anderson BT, Tucker CJ (2003) *Geophys Res Lett*, doi:10.1029/2003GL017506.34.
31. Dai A, Trenberth KE, Qian T (2004) *J Hydrometeorol* 5:1117–1130.
32. Thoning KW, Tans PP, Komhyr WD (1989) *J Geophys Res Atmos* 94:8549–8565.